Environ Sci Technol 1999 33 2163–2169

Mineral Associations and Average Oxidation States of Sorbed Pu on Tuff

M C DUFF,*† D B HUNTER,† I R TRIAY,‡ P M BERTSCH,† D T REED,§ S R SUTTON,∥⊥ G SHEA-MCCARTHY,∥ J KITTEN,‡ P ENG,∥ S J CHIPERA,‡ AND D T VANIMAN‡

Advanced Analytical Center for Environmental Sciences, Savannah River Ecology Laboratory, The University of Georgia, Drawer E, Aiken, South Carolina 29802, Los Alamos National Laboratory, Los Alamos, New Mexico 87545, Chemical Technology, Argonne National Laboratory, Argonne, Illinois 60439, Department of Geophysical Sciences and Center for Advanced Radiation Sources, The University of Chicago, Chicago, Illinois 60637, and Department of Applied Sciences Brookhaven National Laboratory, Upton, New York 11973

Subsurface transport of groundwater contaminants is greatly influenced by chemical speciation, precipitation, and sorption processes The transport of Pu potentially released from spent nuclear fuel disposal and storage sites will be dependent on its interaction with mineral surfaces and speciation in the subsurface The sorption of dissolved Pu(V) on a natural zeolitic tuff that was equilibrated with synthetic groundwater was examined using synchrotron-based microanalytical techniques The tuff contained trace quantities of smectites and iron and manganese oxides, which are present as fracture fill and pore space materials Synchrotron-based micro-X-ray fluorescence (SXRF) showed that Pu is predominately associated with manganese oxides (rancieite) and smectites but not with iron oxides (hematite) In situ micro-X-ray absorption near-edge structure (XANES) spectroscopy measurements on two highly enriched regions (~10 × 15 μm^2) of Pu indicated that the average oxidation state of sorbed Pu was (+V) in one region and (+VI) in the other The observed heterogeneous speciation of the sorbed Pu demonstrates the complex nature of this process Thermodynamic equilibrium calculations indicated that the solution was dominated by negatively charged Pu species (such as $PuO_2CO_3^-$), suggesting that sorption to the negatively charged manganese oxide surfaces would be energetically prohibited Subsequent speciation changes upon sorption to manganese oxide surfaces are discussed

Introduction

Plutonium (Pu) is a key component of spent nuclear fuel that requires careful strategies for environmentally safe management and long term geologic storage One proposed disposal site is the lower portion of the Topopah Spring Member of the Paintbrush tuff unit in Yucca Mountain (YM, NV) Studies on the redox and speciation chemistry of Pu in synthetic and natural waters suggest that Pu can be present in four oxidation states (III, IV, V, and VI) concurrently (*1*) The potential for coexisting valence states and the large differences in complexation behavior and solubility of these oxidation states make the environmental redox chemistry of Pu complex The solubility and mobility of Pu in natural waters vary greatly, with the III and IV valences being notably more sorptive and less soluble because of their high charge The higher valences of Pu(V) and Pu(VI) are less charged because their free ions exist as dioxo moieties $Pu(V)O_2^+$ and $Pu(VI)O_2^{2+}$ (*1–7*) Under acidic conditions, Pu(V) ions disproportionate to Pu(IV) and Pu(VI) (*1*) However, Pu(V) tends to dominate Pu speciation in oxic neutral to basic natural waters and synthetic YM groundwaters (*1, 8–10*)

Studies on the Pu sorption from solutions with known oxidation states on particulates tuff and tuff minerals, characterized soils and sediments and homogeneous solids such as clays and metal oxides, have been performed (*2–4, 7 9 11–16*) The sorption of Pu (added as Pu(IV or V)) on iron oxides and marine sediment particulates is independent of ionic strength and irreversible, suggesting that Pu sorption involves inner-sphere or specific adsorption processes rather than ion exchange or outer-sphere processes (*2–4*) Specific adsorption behavior has been observed with actinides on clay and rock minerals (*7 13–17*) Studies with dissolved Pu(V) show that Pu sorbs *strongly* to smectites and to manganese and iron oxyhydroxide minerals, which can mediate redox transformations (*2, 7, 15 16*) Hence, the sorption of Pu(V) to redox reactive solids may involve the oxidation of Pu(V) to Pu(VI) and the reduction of Pu(V) to Pu(III and IV) (*2–7 9–12*) In synthetic YM groundwaters, all oxidation states of Pu sorb on YM tuffs and synthetic tuff minerals, particularly on iron oxides (*7, 15*) This is somewhat unexpected because neptunium(V) (Np) and uranium(VI) (U) used as analogues of dissolved Pu(V) and Pu(VI) (respectively), sorb poorly on natural YM tuffs and tuff minerals (*7, 15*) The sorption of actinides on YM tuffs enriched with natural iron oxides was no greater than sorption to similar YM tuffs depleted in natural iron oxides suggesting that these oxides were possibly passive to sorption (*7*) Direct in situ spectroscopic measurements of the oxidation state of sorbed Pu species on surfaces are limited Some sorption studies with surfaces assume that the measured or predicted oxidation state speciation of Pu in solution is representative of the oxidation state of sorbed Pu (*2, 3, 9, 12*) These indirect interpretations about speciation may not represent the oxidation-state speciation of sorbed Pu, particularly when the surface can influence the redox chemistry of the Pu

This study investigated sorbed Pu (added as dissolved Pu(V)) on a natural heterogeneous material (tuff) using in situ spatially resolved synchrotron micro-X-ray fluorescence (micro-SXRF) and micro-X-ray absorption near-edge structure (micro-XANES) spectroscopies These analytical methods complement ex situ surface characterization methods for spatially distributed sorbed Pu such as microautoradiography We obtained information on the average oxidation state of sorbed Pu on tuff on a small spatial scale (about 140 μm^2)

Micro SXRF spectroscopy can be used to produce images of elemental distributions on a microscopic level and therefore is an excellent technique for determining the microdistributions of sorbed Pu among various mineral phases in tuff material Once identified by SXRF imaging,

* Corresponding author phone (803)725 7237, fax (803)725 3309, e mail martine@srel edu
† The University of Georgia
‡ Los Alamos National Laboratory
§ Argonne National Laboratory
∥ The University of Chicago
⊥ Brookhaven National Laboratory

10 1021/es9810686 CCC $18 00
Published on Web 05/20/1999

TABLE 1 Thermodynamic Data for Aqueous Pu(V) and Np(V) Solution Species and the Corresponding Solution Species Distribution Percentages for Np(V) and Pu(V) in the Synthetic Carbonate Water

species	β_{xyz}[a]	% Pu or Np species in groundwater	ref
PuO_2^+	NA	2	NA
PuO_2OH^0	$\beta_{1(-1)0} = 10^{-9.73}$	<1	22
$PuO_2CO_3^-$	$\beta_{101} = 10^{5.12}$	98	22
NpO_2^+	NA	9	NA
NpO_2OH^0	$\beta_{1(-1)0} = 10^{-11.3}$	8	23
$NpO_2(OH)_2^-$	$\beta_{1(-2)0} = 10^{-23.43}$	<1	23
$NpO_2CO_3^-$	$\beta_{101} = 10^{4.38}$	74	23
$NpO_2(CO_3)_2^{3-}$	$\beta_{102} = 10^{6.55}$	9	23
$NpO_2(CO_3)_3^{5-}$	$\beta_{103} = 10^{6.4}$	<1	23

[a] $\beta_{xyz}=[M_xH_yL_z]/[M]^x[H]^y[L]^z$ or $\beta_{x(-y)z} = [M_x(OH)_yL_z][H]^y/[M]^x[L]^z$. NA is nonapplicable

isolated regions of Pu enrichment may be probed with micro XANES and extended-X-ray absorption fine structure (EXAFS) techniques Hence, measurements of the bonding environment of particular species on individual mineral microphases can be made on these materials In situ micro-XANES and -EXAFS techniques have been previously utilized to study the local molecular bonding environments of metal contaminants in heterogeneous environmental systems on the micrometer scale (*18, 19*)

Experimental Procedures

Samples Tuff core samples were taken from the USW SD 9 borehole at the 446 8–446 9 m depth at the zeolitized base of the Topopah Spring Tuff at YM This horizon has been identified as a possible barrier to radionuclide transport within the proposed YM high-level waste repository site Core samples were used to prepare polished 30-μm thin sections (*16*) Scanning electron microscopy/energy-dispersive X-ray (SEM/EDX) analyses were conducted on the core material (CM) (*16*) The CM was also examined by quantitative X-ray diffraction (XRD) to determine the abundance of major and minor minerals, trace minerals were identified and characterized by optical petrography combined with SEM and XRD of hand-picked separates (*16*)

Sorption Experiments. A synthetic groundwater (UE-25p#1) (carbonate alkalinity of 11 mequiv L^{-1} as $NaHCO_3$ and Na_2CO_3, pH 8 9) representative of the deep carbonate aquifer below the proposed repository area was prepared (*16*) Water representative of the tuffaceous aquifer has been used in other studies, in some aspects, the carbonate aquifer may be more representative of unsaturated-zone waters ^{239}Plutonium(V) was added from a 10^{-4} M Pu(V) stock solution to the synthetic water to give a final concentration of 10^{-6} M ^{239}Pu(V) (*20*) The 10^{-4} M Pu(V) stock solution was prepared electrochemically and confirmed spectrophotometrically (569 nm, $\epsilon = 19\ M^{-1}\ cm^{-1}$, *20*) The thermodynamic speciation for Pu(V) and analogous Np(V) species were calculated for the synthetic, Pu-containing groundwater with the computer program MINTEQA2, the Davies Equation and a modified database (Table 1, *21–24*)

Two thin sections (TS1 and TS2) were equilibrated by immersion in 20 mL of this freshly prepared synthetic groundwater in the dark for 24 h A third section (TS3) was equilibrated similarly, but for a 120-h period and after the first 24-h equilibration, the solution was changed every 12 h Following equilibration, the thin sections were rinsed with deionized water and allowed to dry in air Thin sections TS1 and TS2 were used for microautoradiography studies (*16*) The activity of sorbed ^{239}Pu on TS1, TS2, and TS3 was determined by a methane gas flow proportional counter Since the α-particles only penetrate 0 5 μm of rock, the quantification of the Pu concentration based on α-particle activity was limited due to the sample geometry The ^{239}Pu activities in the solutions were determined by liquid scintillation counting for TS1, TS2, and TS3 before and after equilibration with the samples Control studies using 10^{-6} M ^{239}Pu solutions in the absence of a thin section were conducted in duplicate to determine the amount of container sorption The amount of sorbed Pu was calculated by difference using the amount of ^{239}Pu activity in the solution before and after equilibration with the thin section The calculations accounted for container sorption (1 4% of the total dissolved Pu added)

In Situ Micro-X-ray Fluorescence Analyses. For the micro-SXRF studies, the synchrotron hard X-ray fluorescence microprobe (beamline X26A) at the National Synchrotron Light Source (Brookhaven National Laboratory, Upton, NY) was used with a channel-cut Si(111) monochromator (*25*) Microfocusing optics were used to produce a small X-ray beam A double elliptical Au-coated Kirkpatrick-Baez mirror system operated at a pitch of 5 mrad was used to focus a 350 by 350 μm^2 monochromatic beam at the Pu L_{III} absorption edge (18054 eV) down to a 10 by 15 μm^2 beam, resulting in a total flux of about 10^{10} photons s^{-1} (*25–27*) TS1 and TS3 were contained within fitted plastic inserts with polypropylene and Kapton windows, placed in a metal frame and mounted on an automated, digital $x-y-z$ stage at 45° to the beam Fluorescent X-rays were detected with a Si(Li) energy-dispersive (EDS) detector (30 mm^2 area) mounted at 90° to the incident beam and about 1 cm from the sample Elemental mappings on TS1 and TS3 were conducted using micro-SXRF spectroscopy at several areas, ranging from 140 by 140 μm^2 to 400 by 400 μm^2 in size For elements with absorption energies below 18 5 keV, SXRF was performed by collecting 20 s live counts in the elemental regions of interest and rastering the sample in 3–10 μm steps in the $x-y$ plane A thin film XRF standard reference material (SRM) from the National Institutes of Standards and Technologies (SRM 1833) that contains known concentrations of Pb was used to make estimates of the Pu concentrations at highly localized areas on the tuff The Pu sensitivity by SXRF relative to Pb was calculated using the software package NRLXRF (*28*)

One complication was the inability to resolve the Pu Lα emission peak (14 28 keV) and the Sr Kα emission peak (14 17 keV) with a Si(Li) EDS detector This problem was circumvented by making two elemental maps of the samples one made with the monochromator energy below the Pu L_{III} absorption edge (excites Sr fluorescence) and one made above the edge (excites Pu and Sr) and then subtracting the images to get the Pu distribution only

In Situ Micro-X-ray Absorption Analyses For micro-X-ray absorption analyses, the X-ray microprobe described above was used, and XANES spectra were acquired in fluorescence mode as the monochromator was scanned through the Pu L_{III} edge The XANES spectra were obtained for two ~10 × 15 μm^2 regions on TS3 that contained the greatest levels of sorbed Pu, as determined by SXRF mapping region 1 (triplicated) and region 2 (duplicated) The XANES spectra were collected from 50 eV below to 100 eV above the Pu L_{III} absorption edge in varying step increments from 0 4 to 2 5 eV Count times varied from 10 s (Pu solid phases) to 240 s (regions 1 and 2 on TS3) per point

The half-height of the edge step for the Pu L_{III} XANES edge energies were defined and normalized to be 0 eV with the most stable and characterized standard, Pu(IV)O_2(s), and were monitored with PuO_2(s) before and after each sample A second standard was $Ba_3Pu(VI)O_6$ The PuO_2 was made from highly purified ^{242}Pu oxide material from Oak Ridge National Laboratory (Oak Ridge, TN) Upon receipt, the oxide was high-fired at 1000 °C at Argonne National Laboratory (Argonne, IL) and analyzed by XRD to confirm its purity (*29,*

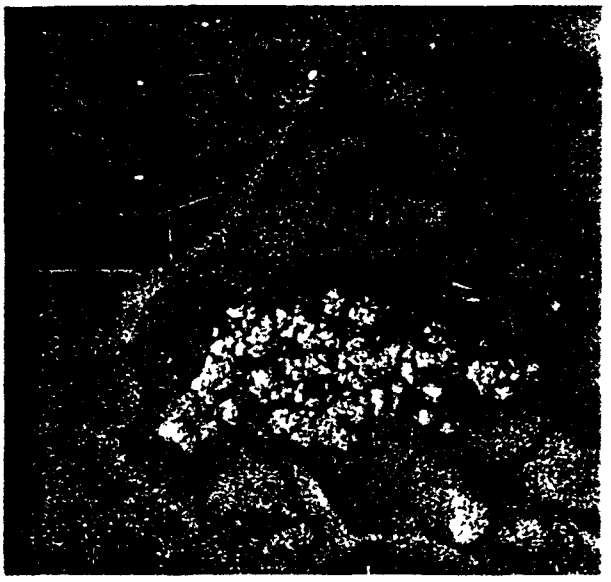

FIGURE 1 Back-scattered electron SEM image of a rancieite–smectite zone in the core material—a surface morphology that resembles areas with elevated Pu sorption (scale bar, 50 μm)

30) The Pu(VI) standard was synthesized in 1982 and characterized by dissolution in dilute acid followed by spectrophotometric analyses of Pu oxidation states (*31*) The Pu(VI) standard was determined to be more than 99 7% Pu(VI) with trace quantities of Pu(IV and V) and was stored in a sealed state in a drybox until use

An increase with respect to the relative XANES edge energy indicates an increase in the average Pu oxidation state in the sample or standard of interest For example, previous studies have shown that a linear relationship exists between the fraction of U(VI) and U(IV) and the edge energy (*18, 33*) A relationship between elemental oxidation state and edge (or pre-edge) energy values has been observed with several non-actinide and actinide elements, including Pu (*18–20, 29, 32*)

Results and Discussion

Solution Speciation Modeling. Oxidation-state determinations of Pu in waters show that Pu(V) becomes the dominant oxidation state of Pu in synthetic and natural UE-25p#1 groundwater from YM when the original source of Pu added was Pu(IV) (*10*) Hence, thermodynamic equilibrium calculations that assumed Pu(V) was the only oxidation state present during the exposure of the Pu to the tuff thin section were conducted The calculations predicted that the dominant Pu(V) species was $PuO_2CO_3^-$ (Table 1, *21–24*) When only one oxidation state of Pu was assumed in the equilibrating solution, calculations for waters containing 10^{-6} M Pu(III, IV, or VI) predicted that greater than 90% of the Pu existed as negatively and neutrally charged carbonate and hydroxide species (thermodynamic data from ref *24*) For comparison, Np(V) was used in the calculations because thermodynamic data for plutonium(V) carbonate species are somewhat scarce and the thermodynamic database for likely neptunium(V) carbonate species is relatively more complete When Np(V) was assumed in the solution, negatively charged neptunium(V) carbonate and hydroxide species were predicted

Characterization of Tuff, Pu Sorption, and Microautoradiography. Qualitative XRD results show that the CM is predominantly zeolitic (clinoptilolite 80 wt %, smectite 2%, opal-CT 8%, feldspar 7%, quartz 3%) Smectite isolates from the CM contained the mineral rancieite $(Ca,Mn^{2+})O\ 4Mn^{4+}O_2\ 3H_2O$ An example of a smectite–rancieite association

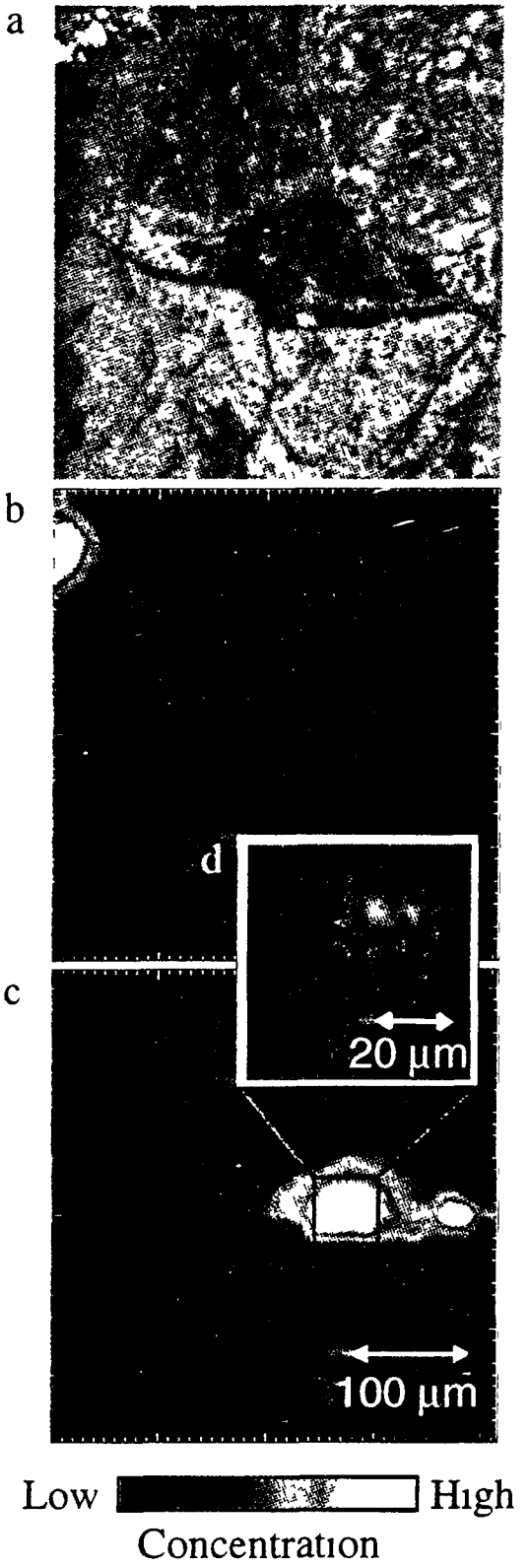

FIGURE 2 (a) Photomicrograph of the manganese and iron oxides phases in area 1 (TS3) under reflected light (scale bar, 100 μm) The silver-colored structure in the upper left corner is hematite, the center area is a manganese oxide, and the surrounding features are highly zeolitic Complementary micro-SXRF elemental map images of panel a showing spatially localized (b) Fe (c) Mn, and (d) Pu

obtained from the CM is shown in Figure 1 Rancieite is an isomorph of birnessite (MnO_2 or $Na_4Mn_{14}O_{27}\ 9H_2O$) (*34, 35*),

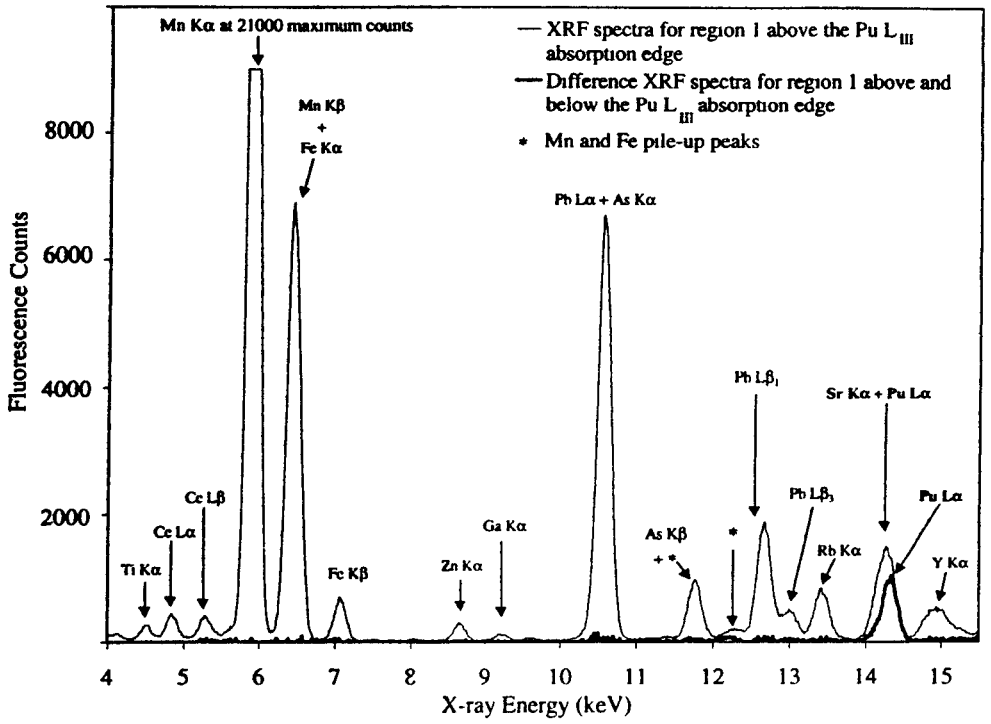

FIGURE 3 SXRF spectra taken at region 1 on TS3

and some researchers consider its structure to be unknown (*34*) It is reported that rancieite has a hexagonal structure with layers of octahedral $[Mn(IV)O_6]^{8-}$ that are separated by interlayer Ca, Mn^{2+}, and H_2O (*34, 35*) The XRD pattern for rancieite is similar to that of birnessite, but the *d*-spacings for some of the rancieite diffraction lines are slightly greater (*35–37*) Rancieite may be a layered mixture of decomposing buserite (an isomorph of birnessite) and birnessite (*34, 37*) More research on the structure of rancieite is needed

Greater than 98% (about 10^{17} ^{239}Pu atoms) of the added Pu(V) was sorbed to TS1 and TS2, and 92% (about 10^{18} ^{239}Pu atoms) of the Pu added was sorbed to TS3 More sorption of Pu on TS3 occurred because the equilibration of TS3 with Pu(V)-containing solution was longer and the solution was changed every 12 h A longer equilibration of TS3 was performed because greater surface loadings of Pu were needed to obtain a suitable signal for Pu in the presence of a high Sr background, which interfered with the fluorescence detection of Pu However, similar α activities were obtained for sorbed Pu on TS1, TS2, and TS3 (about 28–29 dpm × 10^3) Microautoradiography studies with TS1 (data not shown) in combination with optical petrographic and XRD techniques indicate that Pu sorbed more strongly to smectite and manganese oxide fracture minerals than to zeolites (*16*) Line-scan mappings of Ag in the exposed and developed microautoradiography emulsion with SEM–EDX on TS1 showed that Ag (precipitated by microautoradiography) was associated with Mn and smectites (*16*) Zeolites and smectites (not including broken edge sites on smectites) sorb by cation exchange or outer-sphere sorption processes whereas iron and manganese oxides generally sorb ions via inner-sphere or specific adsorption processes If significant sorption of Pu to zeolites or smectites occurred, one would anticipate outer-sphere sorption, but this was not observed in microautoradiography studies, batch sorption studies, or in this study (*7, 16*)

SXRF Analyses of Sorbed Pu on Tuff The two selected areas on TS3 contained iron and manganese oxide bodies that were present as fracture fill minerals in a predominantly zeolitic region (Figures 2a–d and 3, data for the second area not shown) A SXRF spectrum for region 1 on the tuff that contained highly elevated sorbed Pu is shown in Figure 3 Elemental mappings of TS1 (with emulsion) and TS3 (without emulsion) showed that As, Ca, Ce, Ga, Nb, Pb, Sr, Ti, Y, and Zn (data not shown) are co-associated with areas with Mn-rich regions (Figure 2a–d) and *not* with Fe On TS1, Ag was also correlated with Mn Iron oxides have strong affinities for Pu, but the hematite surfaces in this sample of tuff appear passivated and inaccessible to sorption—as observed in other sorption studies with iron oxides in YM tuff (*7*) This passivation may be due to surface coatings of silica, carbonate, or possibly organic matter on the iron oxides (*38*) Little work has been done with these surface coatings on manganese oxides, and it is not understood why the manganese oxides are not equally passivated The data suggest that Pu and several elements are co-associated with manganese oxide–smectite associations and not with hematite (Figures 2b–d and 3) Rancieite from YM is often enriched in Ca, Ce, Pb, Sr, Ti, Y, and Zn, and these mappings concurred with semiquantitative results from SEM–EDX studies with rancieite isolates from YM (*39*) With the exception of As, which is usually present in the environment as an anionic species, the elements associated with the rancieite on the tuff exist as cations ($Ce^{3+/4+}$, Ca^{2+}, Ga^{3+}, Nb^{4+}, Pb^{2+}, Sr^{2+}, Ti^{3+}, Y^{3+}, and Zn^{2+}) in solution These elements may be interlayer cations, sorbed species, surface precipitates, and possibly isomorphically substituted cations in the rancieite and smectite Using semiquantitative SXRF measurements based on known concentrations of Pb in rancieite from YM and thin film standards, about 1 g of Pu (kg of tuff)$^{-1}$ was calculated to be present in the spatially localized regions of sorbed Pu (*18, 25*, data on Pb concentrations in rancieite from ref *39*)

A highly simplified approach was performed to calculate whether monolayer coverage of sorbed Pu on the manganese oxide and smectite was possible—based on 20 mineral bodies (of birnessite and smectite) 0 0135 mm^3 in size (data not shown, mineral surface data from ref *40*) present on the thin section Rancieite phases were unavailable for surface

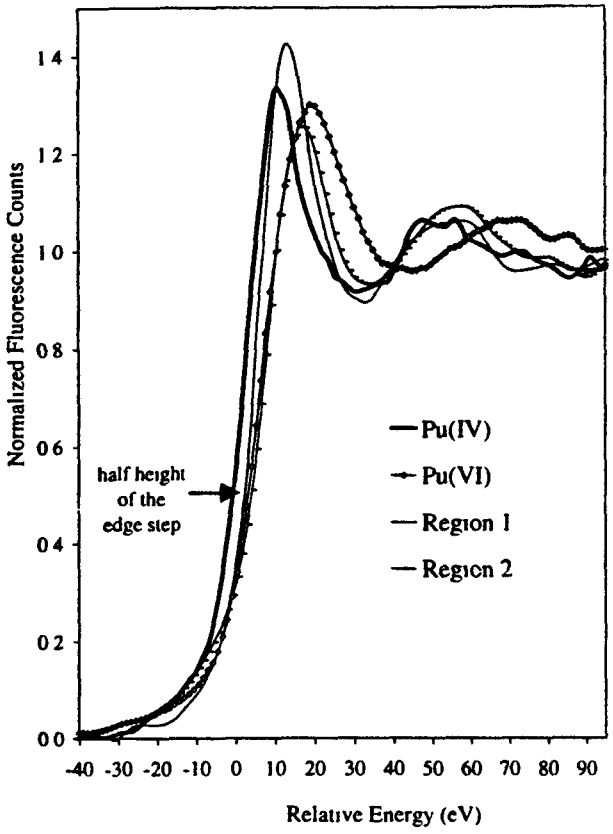

FIGURE 4 Pu-XANES spectra for the standards (Pu(IV) and (VI)) and regions 1 and 2 on the tuff demonstrating the edge energy shift with oxidation state at the half-height of the edge step as labeled with an arrow The average edge energy for TS3 (region 1) is slightly more than midway between Pu(IV) and Pu(VI), which based on relative edge energy, would be consistent with a Pu(V) species (*20, 29*) Small amounts (submicrograms) of Pu standards were encapsulated in polystyrene for ease of handling and safety during the analyses

measurements, so birnessite was used The estimated number of surface sites present on these minerals was within an order of magnitude of the number of Pu atoms sorbed to TS1 and TS3, suggesting that monolayer coverage of sorbed Pu is possible However, more detailed sorption and modeling studies with a variety of controlled conditions (pH, Pu solution concentration and surface coverage, etc) are needed to better characterize Pu(V) sorption on natural minerals in the tuff The specificity of Pu sorption suggests that multiple binding sites are present on the manganese oxide–smectite phases Some specific adsorption may have occurred at broken edge sites on smectite, as has been observed with U(VI) (*17*)

XANES Analyses of Sorbed Pu on Tuff In the XANES analyses, the energy of the X-ray absorption edge increases with increasing valence—a result associated with reduced shielding of the core electrons This increase in the binding energy of the core levels is often manifested by systematic shifts in the preedge and bound-state features in a XANES spectrum, which can be correlated to differences in the oxidation state of a cationic center (*18, 19, 25, 32, 33, 41*) The average fluorescence values for the XANES edge energies of the standards were 0 eV for Pu(IV) and +3 0 eV for Pu(VI) (Figure 4) These analyses compared well with edge energy shift values from XANES studies of solutions and solids with known Pu oxidation states (*20, 29*) and studies using solutions and solids of U(IV) and U(VI) (*18, 33, 41, 42*) The relative Pu edge energy shift for TS3 on region 1 ranged from +1.3 to +2 0 eV, with a mean value of 1 7 ± 0 4 eV This corresponds to an average oxidation state of mostly +V Sorbed Pu at region 1 may be present on the manganese oxide–smectite surface as Pu(V) or a mixture of Pu(IV and VI) (Figure 4) At region 2 on TS3, the relative edge energy shifts were +2 6 and +3 4 eV (a mean of 3 0 ± 0 6 eV), which is indicative of primarily Pu(VI) (Figure 4) Similar results were obtained for a least-squares method for fitting the XANES data with an arctangent function and a Gaussian function where the edge was defined as the inflection point of the arctangent function (*20, 29*)

Post-edge structural features associated with multiple scattering resonances, provide qualitative information on the nearest neighbor coordination and bonding environment For example, actinide(V) and -(VI) solution species usually have axial O bonds such as the $Np(V)O_2^+$, $Pu(V)O_2^+$, $Pu(VI)O_2^{2+}$, and $U(VI)O_2^{2+}$ ions (*20, 43*), and these species tend to have post-edge resonance spectral features that resemble a "shoulder" on the high energy side of the main absorption feature or white line However, the post-edge spectra for sorbed Pu on regions 1 and 2 on the tuff lack this shoulder There are several possible explanations for the absence of this feature First, the height of the white line may have diminished the contribution of the multiple scattering resonances to the post-edge spectra Second, the sorbed Pu at region 1 may exist as Pu(IV and VI) or Pu(IV, V, and VI) with the XANES post-edge spectral features representing an average of these oxidation states In this manner, the overlap of the spectra for these possible oxidation states could result in a broadened shoulder feature Third, the absence of the shoulder could be a result of the bonding geometry The absence of a shoulder has been observed for sediments with mostly U(VI), sediments containing recently oxidized U(IV), uranates and U(V) containing glasses (*41 42, 44 45*), and it has been attributed to lengthening of the axial actinide–O bond (*20 45*) The axial O bond distance observed for U(VI) in schoepite in aqueous solution is 1 80 Å at pH 7 and lengthens to 1 86 Å at pH 11 when the formation of uranates (which contain U(VI), such as Na_2UO_4) is favored (*45*) The presence of a post-edge resonance feature in the XANES spectra cannot be used as an indicator of V and VI oxidation states for Pu and U (*41, 44, 45*) This feature is more related to the bonding and coordination environment around the actinide atom (*41 45*) The influence that coordination geometry (such as the absence of axial O bonds) may have on the XANES edge energy values is worthy of investigation The relative XANES edge energy value that we obtained for our Pu(VI) standard, which does not have axial O bonds compared well with that obtained for solution Pu(VI) species which do have axial O bonds This finding demonstrates that oxidation state rather than coordination geometry is the dominant factor influencing the XANES edge energy

One of the main results of this work is that sorption of Pu to tuff is primarily at manganese oxide and smectite bodies with subsequent heterogeneity in Pu oxidation state Region 2 has been interpreted as containing Pu(VI), requiring some mechanism to oxidize the solution Pu(V) One possibility is an electron exchange process between Pu and Mn The Mn(IV) (in rancieite) may have oxidized Pu(V) to Pu(VI) becoming reduced to Mn(III) or, in the case of excess Pu(V), to Mn(II) in the process The manganese oxides can promote the oxidation of many transition metals (*38, 46*) The average zero point of net charge values for rancieite are unknown but are about 1 5 for birnessites, indicating that they are highly negatively charged (*34*) The preferential sorption of Pu to manganese oxides that are dominated by negatively charged sites suggests that positively charged Pu species are attracted to the tuff surface Thus, the calculated equilibrium speciation for dissolved Pu species is not representative of the distribution of sorbed Pu species on

5

the surface, and it cannot provide conclusive interpretations about the redox behavior of sorbed Pu The speciation of sorbed Pu on surfaces should be more influenced by solid–water interfacial processes than by the *equilibrium* speciation of dissolved Pu

Fundamental experiments on redox reactions with sorbed Pu on natural manganese oxides are needed to further investigate these findings Such research needs to be systematically conducted with Pu on a variety of characterized homogeneous mineral surfaces (for example, on various iron and manganese oxides) in a variety of waters The investigation of Pu sorption on homogeneous surfaces would complement other research with natural heterogeneous solids Moreover, the application of nondestructive in situ speciation methods such as micro-XANES, -EXAFS,-Raman, diffuse-reflectance micro-infrared, and possibly electron energy-loss spectroscopy of sorbed Pu on these kinds of surfaces should elucidate the mechanisms of Pu–surface interactions However, the application of many in situ micro-spectroscopic techniques to the characterization of Pu sorption on natural, heterogeneous systems is at the preliminary stages of development Although the oxidation state information presented is not entirely conclusive for region 1 on the tuff, the results invoke progressive questions about Pu sorption chemistry at the natural solid–water interface For example, we observed that Pu was not sorbed strongly to iron oxides in this natural system A thorough investigation of this phenomenon is needed Additional spectroscopic information on sorbed Pu at homogeneous surfaces and in mixed phase systems would benefit our understanding of Pu sorption processes

In conclusion, the spatial distribution and the XANES spectra of sorbed Pu demonstrated that Pu is sorbed strongly and preferentially to manganese oxides and not to iron oxides or zeolites in this YM tuff Localized regions of Pu enrichment were identified with variable average Pu oxidation state, Pu(V) and Pu(VI) Without the use of the microprobe, these observations would not be possible Our findings indicate that the study of Pu sorption on heterogeneous redox reactive surfaces is a function of the environment at the heterogeneous solid–water interface rather than of the solution speciation

Acknowledgments

This research was supported by Financial Assistance Award DE-FC09-96SR 18546 from the U S Department of Energy to the University of Georgia Research Foundation, by laboratory-directed funds at Argonne National Laboratory and by the Yucca Mountain Project (YMP) as part of the Civilian Radioactive Waste Management Program and is managed by the U S DOE, YMP The X26 microprobe beamline is supported in part by DOE Grant DE-FG02-92ER14244 (S R S) We thank L. Morss for the Pu(VI) solid, M Neu for the Pu(V) stock solution, and NSLS staff for assistance

Literature Cited

(1) Choppin, G R , Bond, A. H , Hromadka, P M *J Radioanal Nucl. Chem* **1997**, *219*, 203–210
(2) Sanchez, A L., Murray, J W , Sibley, T H *Geochim Cosmochim Acta* **1985**, *49*, 2297–2307
(3) Keeney-Kennicutt, W L., Morse, J W *Geochim Cosmochim Acta* **1985**, *49*, 2577–2588
(4) McCubbin, D , Leonard, K S *J Radioanal. Nucl Chem Art* **1993**, *172*, 363–370
(5) Nelson, D M , Lovett, M B *Nature* **1978** *276*, 599–601
(6) Cleveland, J M In *The Chemistry of Plutonium*, Gorden and Breach Science New York, 1971
(7) Triay, I R , Meijer, A., Conca, J L., Kung, K S , Rundberg, R S , Strietelmeier, E A., Tait, C. D *Summary and Synthesis Report on Radionuclide Retardation for the Yucca Mountain Site Characterization Project* Yucca Mountain Site Characterization Program LA-13262 MS 1997
(8) Peretrukhin V F , David F , Maslennikov A. *Radiochim Acta* **1994** *65* 161–166
(9) Boust, D Mitchell P I Garcia K Condren O Leon Vintro L., Leclerc G *Radiochim Acta* **1996** *74* 203–210
(10) Nitsche H Roberts K Prussin T , Muller A. Becraft K Keeney D , Carpenter S A , Gatti R C *Measured Solubility and Speciation Studies from Oversaturation Experiments of Neptunium Plutonium and Americium in UE-25p#1 Well Water from the Yucca Mountain Region* Yucca Mountain Site Characterization Program LA-12563-MS, 1994
(11) Kaimin E P , Konstantinova L I *Radiochemistry* **1996** *35* 360–364
(12) Penrose, W R , Metta D N Hylko J M Rinckel L A. *J Environ Radioanal* **1987** *5* 169–184
(13) Berry J A Bishop H E. Cowper M M Fozard P R , Mcmillian J W Mountfort S A *Radiochim Acta* **1994** *66* 7, 243–250
(14) Means J L Crerar D A Borcsik M P , Duguid J O *Geochim Cosmochim Acta* **1978** *42* 1763–1773
(15) Lu N , Cotter C R Kitten H D , Triay I R *Iron Oxide Colloid Facilitated Plutonium Transport in Ground Water* Pu Futures Los Alamos National Laboratory Santa Fe NM August 1997
(16) Vaniman D T Furlano A Chipera S Thompson J Triay I R *Mater Res Symp Proc.* **1996** *412*, 639–646
(17) McKinley J P Zachara J M Smith, S C Turner G P *Clays Clay Miner* **1995** *43*, 586–598
(18) Bertsch P M , Hunter D B , Sutton S R Bajt S Rivers M L. *Environ Sci Technol* **1994**, *28* 980–984
(19) Tokunaga T K Brown G E Pickering I J Sutton S R Bait S *Environ Sci Technol* **1997**, *31* 1419–1425
(20) Conradson S D , Al Mahamid I Clark, D L. Hess, N J Hudson E A. Neu M P , Palmer P D Runde, W H Tait C D *Polyhedra* **1998** *17* 599–602
(21) U S EPA *Metal Speciation Equilibrium Model for Surface and Groundwater*, Version 3 11 CEAM-USEPA Athens, GA 1991
(22) Bennett D A., Hoffman, D Nitsche H , Russo R E , Torres R A. Baisden, P A. Andrews, J E Palmer C E Silva R J *Radiochim Acta* **1992** *56* 15–19
(23) Banaszak, J E , Reed D T , Rittman, B E *Environ Sci Technol* **1998** *32*, 1085–1091
(24) Lemire, R J , Tremaine, P R *J Chem Eng Data* **1980** *25*, 361–370
(25) Smith J V , Rivers M L In *Synchrotron X ray Microanalysis in Microprobe Techniques in the Earth Sciences* Potts, P J , et al Eds , Chapman and Hall London 1995 pp 163–233
(26) Eng P J , Rivers, M L , Yang B X., Schildkamp, W *Proc SPIE* **1995**, *2516* 41–51
(27) Yang B X. Rivers M L. Schildkamp, W , Eng P *Rev Sci Instrum* **1995** *66* 2278
(28) Criss J W *NRLXRF, A FORTRAN Program for X ray Fluorescence Analysis, User s Reference Manual and Documentation* Naval Research Laboratory Washington, DC 1977
(29) Kropf A J Reed, D T , Aase, S B *J Synchrotron Radiat* (in review)
(30) Reed, D T Kropf A J Aase S B To be submitted to *Environ Sci Technol*
(31) Gens, R , Fuger, J , Morss L R , Williams C W *J Chem Thermodyn* **1985** *17* 561–573
(32) Brown G E , Jr Calas, G Waychunas, G A., Petiau, J In *Reviews in Mineralogy*, Vol 18, Hawthorn, F C , Ed , Mineralogical Society of America Chelsea, MI 1988 pp 431–512
(33) Giaquinta, D M , Soderholm, L., Yuchs, S E , Wasserman S E *Radiochim Acta* **1997**, *76* 113–121
(34) McKenzie, R M In *Minerals in Soil Environment* 2nd ed Soil Science Society of America Book Series Dixon J B , Weed S B , Eds , Soil Science Society of America Madison WI 1989 pp 439–465
(35) Kim, S J *J Mineral Soc Kor* **1993**, *3*, 34–43
(36) Lind, C J , Hem, J D *Appl Geochem* **1993**, *8*, 67–80
(37) Perseil, E A. Giovanoli R *La "rancieite du gisement ferro manganesifere de Rancie (Pyrenees Ariegeoises)*, La Genese des Nodules de Manganese 289 Lalou, C Ed Colloques International du Centre National de la Reserche Scientifique France 1978, pp 369–377
(38) Jenne, E A. Molybdenum in the Environment In *Trace element sorption by sediments and soils–Sites and processes* Chappel W , Petersen K. Eds , Marcel Dekker New York 1977, pp 425–553
(39) Carlos, B A Chipera, S J , Bish, D L , Craven, S J *Chem Geol* **1993**, *107*, 47–69

(40) Langmuir D In *Aqueous Environmental Geochemistry* Prentice Hall Englewood Cliffs, NJ, 1997, p 345
(41) Farges, F, Ponader, C W, Calas, G, Brown, G E., Jr *Geochim Cosmochim. Acta* **1992**, *56*, 4205–4220
(42) Duff, M C, Amrhein C, Bertsch P, Hunter D B *Geochim. Cosmochim Acta* **1997**, *61*, 73–81
(43) Allen, P G, Bucher, J J, Shuh, D K., Edelstein N M, Reich T *Inorg Chem.* **1997**, *36*, 4676–4683
(44) Duff, M C, Hunter, D B, Bertsch, P M, Amrhein C *Biogeochemistry* **1999**, *45*, 95–114
(45) Allen P G Shuh D K Bucher J J Edelstein N M Palmer P A Silva R J Nguyen S N, Marquez L N Hudson E A *Radiochim. Acta* **1996** *75* 47–53
(46) Stumm W In *Chemistry of the Solid–Water Interface* Wiley New York, 1992 pp 323–335

Received for review October 14, 1998 Revised manuscript received April 14, 1999 Accepted April 21, 1999

ES9810686